EURCOLD

eDF

Cfbr FrenchCold

International Workshop on overflowing erosion of dams and dikes

11 – 14th December 2017 - AUSSOIS, FRANCE

CONCRETE DAMS OVERTOPPING EROSION

Session 6: State of the Art Part - 1

Technical University of Cartagena Research
Paute Cardenillo and Toachi Dams

Prof. Luis G. Castillo, PhD
José M. Carrillo, PhD

Hidr@m Group. Department of Civil Engineering.
Universidad Politécnica de Cartagena

Universidad Politécnica de Cartagena

EICM ETS de Ingeniería de Caminos, Canales y Puertos y de Ingeniería de Minas

Hidr@m

PLUNGE POOLS

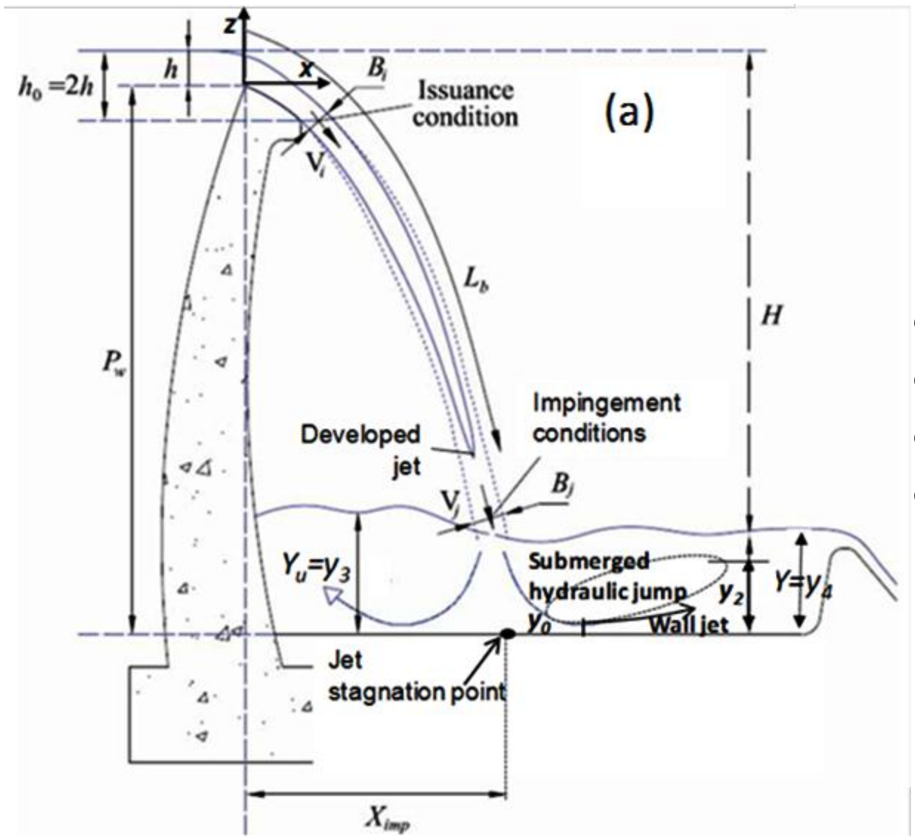

- ❑ Energy dissipation mechanisms can be grouped into the following:

- ○ Aeration and disintegration of the jet in its fall,
- ○ Air entrainment and diffusion into the basin,
- ○ Impact on the basin bottom,
- ○ Recirculation in the basin.

Technical University of Cartagena Research

Turbulent Jet Experimental Facility

- Falling height: 2.20, 2.85 and 3.50 m
- Flows: 10 - 150 l/s
- Inlet channel: 4.10 m length and 1.10 m width
- Plunge pool: 1.3 m high, 1.1 m width and 3.0 m long

Measurements of the principal hydraulics variables:

- Instantaneous pressures (piezoresistive transducers)
- Instantaneous velocities (ADV)
- Mean velocities and air concentrations (Optical fiber)
- Mean velocities (LS-PIV)

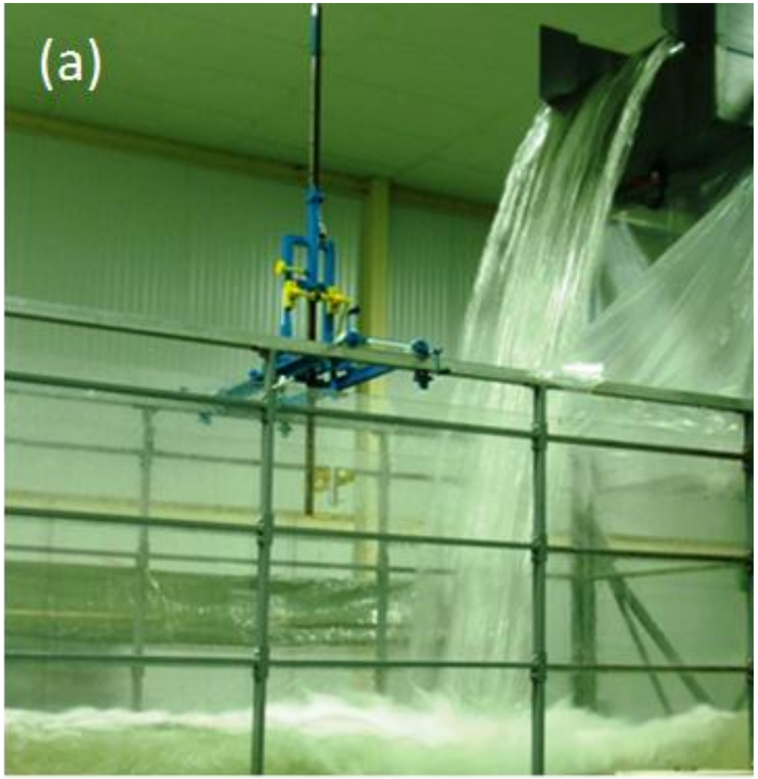

Computational Fluid Dynamics (CFD)

- ANSYS CFX
- FLOW-3D

Velocity and aeration measurements
- In the air

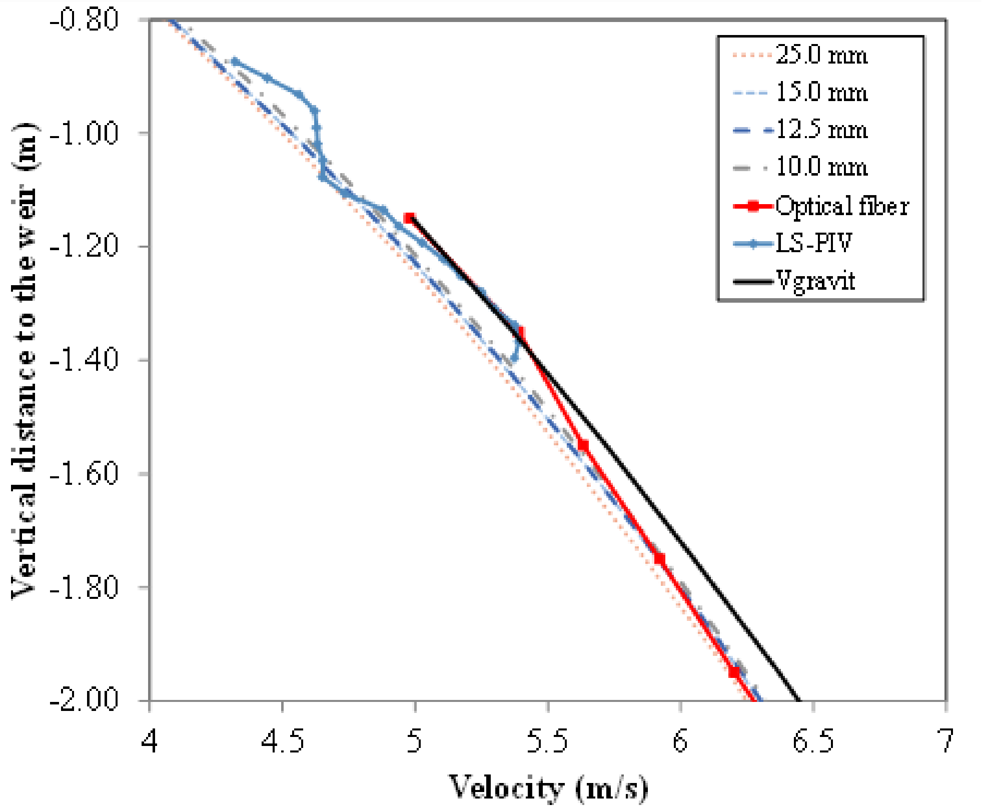

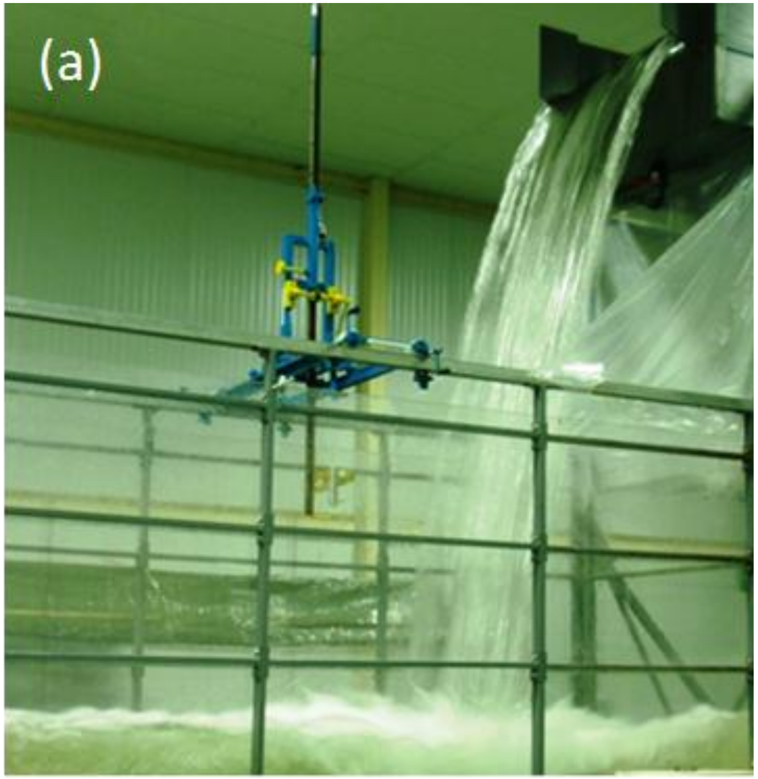

Carrillo, J.M., Castillo, L.G., Marco, F. & García, J.T. (2018). 7th International Symposium on Hydraulic Structures. Aachen, Germany, 15-18 May.

Jet break-up length L_b:

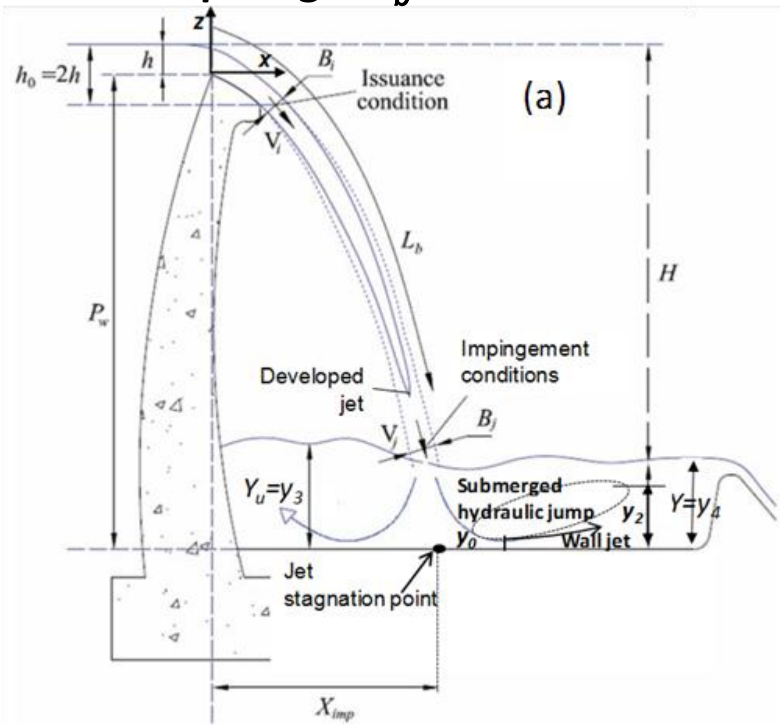

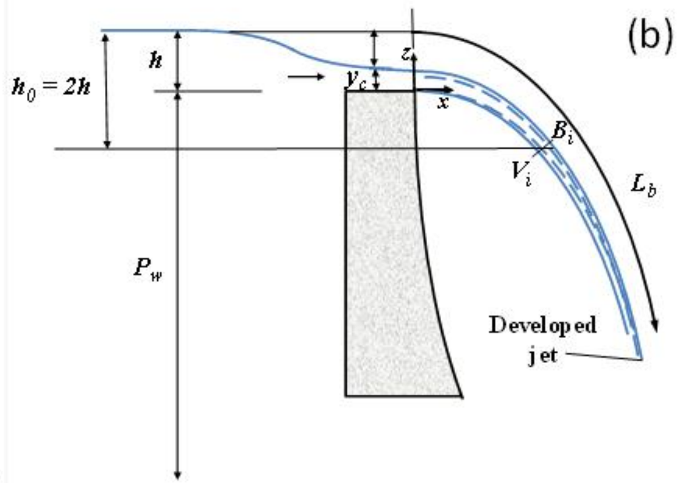

$$\frac{L_b}{B_i F_i^2} = \frac{K}{\left(\varphi F_i^2\right)^{0.82}} = \frac{C_d^{0.82} h^{0.73}}{2g^{0.68}\varphi^{0.82}} K$$

B_i and F_i: thickness and Froude number in issuance conditions.

K: coefficient. Arch dam (inclined crest) ~ 0.85; Gravity dam (flat crest) ~ 0.95

$\varphi = K_\varphi T_u$: turbulence parameter. Arch dams: T_u ~ 0.012, K_φ ~ 1.24, C_d ~ 2.1

Gravity dams: T_u ~ 0.013, K_φ ~ 1.20, C_d ~ 1.7

Castillo, L.G., & Carrillo, J.M. (2016). Pressure and Velocity Distributions in Plunge Pools. Protections 2016 . Ft. Collins, Colorado, USA, 7-9 September.

Impimgement jet thickness

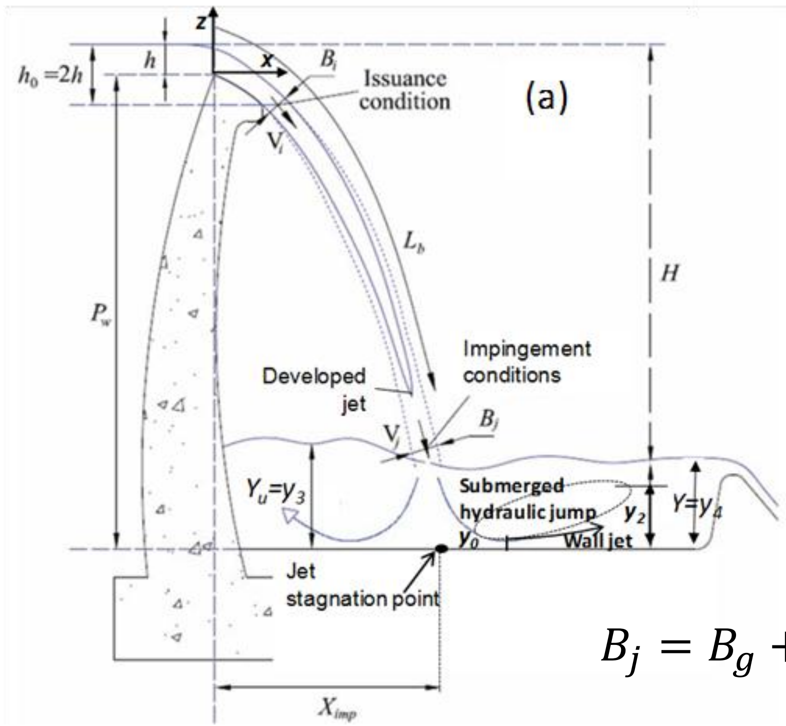

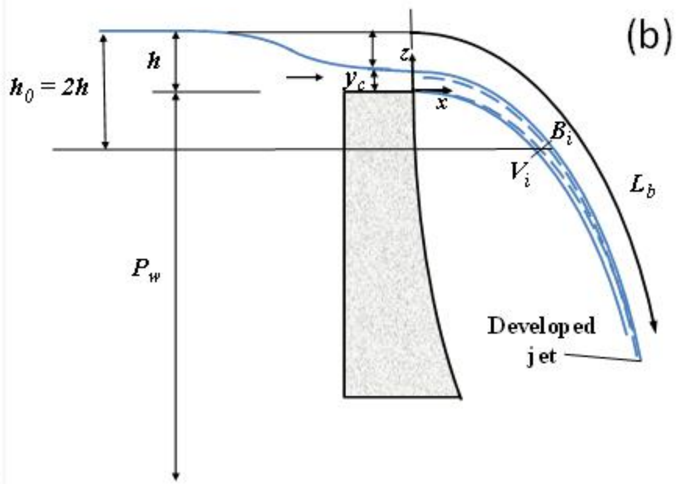

$$B_j = B_g + 2\xi = \frac{q}{\sqrt{2gH}} + 4\sqrt{h}\left(\sqrt{2H} - 2\sqrt{h}\right)$$

B_g: thickness due to gravity (9.8 m/s^2),
ξ: symmetric jet lateral spreading due to turbulence and aeration effects (m),
q: specific flow (m^2/s),
h: weir head (m); H: total head (m).

In the basin

Two principal eddies produce dominant frequencies in plunge pool: large scale eddies and shear layer structures (Ervine and Falvey, 1987).

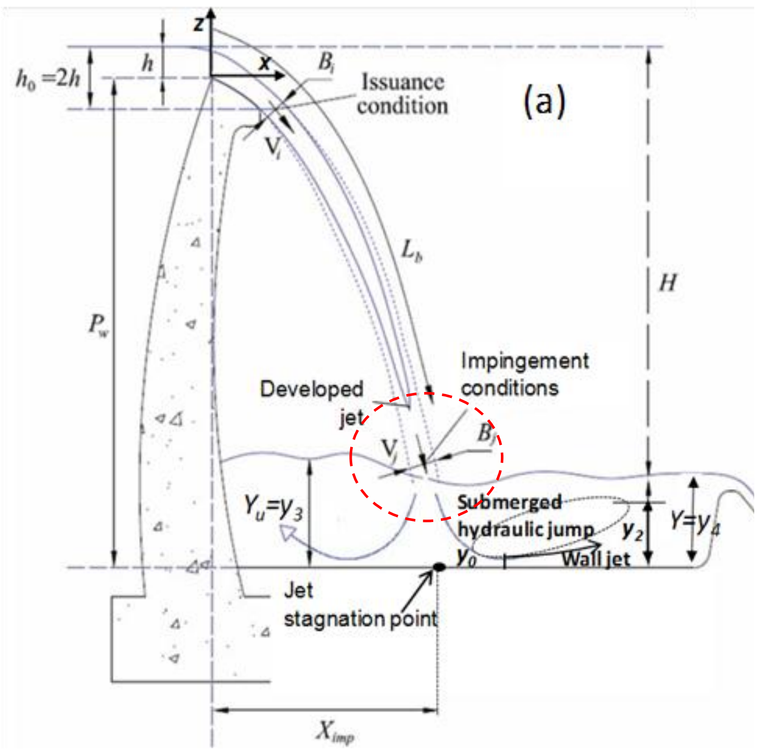

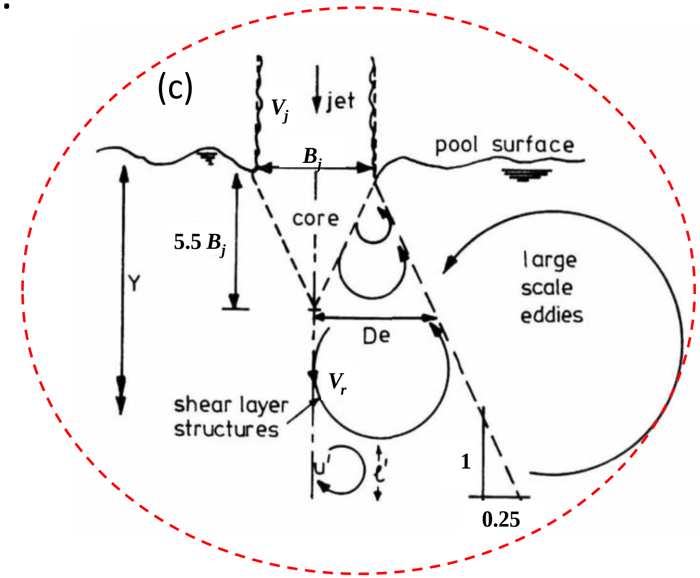

- **Energy dissipation in the basin by diffusion effects** can only be produced if there is an **effective water cushion**:

  Rectangular jet: $Y/B_j > 5.5$

  Circular jet: $Y/B_j > 4$

Dynamic pressures: in function of H/L_b and Y/B_j ratios.

Total dynamic pressure: $$P_{total} = C_p\left(\frac{Y}{B_j}\right)P_{jet} + C_p{}'\left(\frac{Y}{B_j}\right)P_{jet}$$

P_{jet}: stream power per unit of area

$C_p(Y/B_j)$ = mean dynamic pressure coefficient $= \frac{H_m - Y}{V_i^2/2g} = ae^{-b\left(\frac{Y}{B_j}\right)}$

Table 3 Parameters of the mean dynamic pressure coefficient for $Y > 5.5B_j$

H/L_b	a	b	R^2
≤0.85	2.50	0.20	0.93
0.90–1.00	1.70	0.18	0.70
1.00–1.10	1.35	0.18	0.85
1.10–1.20	1.05	0.18	0.95
1.20–1.30	0.88	0.18	0.85
1.30–1.40	0.39	0.15	0.76
1.40–1.60	0.24	0.14	0.68
≥1.60	0.14	0.12	0.56

Castillo, L.G., Carrillo, J.M. & Blázquez, A. (2014). Plunge pool dynamic pressures: a temporal analysis in the nappe flow case. Journal of Hydraulic Research, DOI: 10.1080/00221686.2014.968226.

$C_p'(Y/B_j)$ = fluctuating dynamic pressure coefficient $= \frac{H'}{V_j^2/2g}$

If $\frac{Y}{B_j} \leq 14$: $C_p' = a\left(\frac{Y}{B_J}\right)^3 + b\left(\frac{Y}{B_J}\right)^2 + c\left(\frac{Y}{B_J}\right) + d$ If $\frac{Y}{B_j} > 14$: $C_p' = ae^{-b\left(\frac{Y}{B_j}\right)}$

Table 4 Parameters for calculating the fluctuating dynamic pressure coefficient

	$0 \leq Y/B_j \leq 14$				$Y/B_j > 14$	
H/L_b	a	b	c	d	a	b
$\leq$ 0.80	0.00030	−0.01000	0.0815	0.080	1.500	0.210
0.80–1.00	0.00030	−0.01000	0.0790	0.130	1.800	0.210
1.00–1.30	−0.000005	−0.00220	0.0160	0.350	1.000	0.150
1.30–1.60	0.00003	−0.00180	0.0100	0.210	0.400	0.120
1.60–1.80	0.00005	−0.00195	0.0098	0.160	1.330	0.230
$\geq$1.80	0.00005	−0.00190	0.0100	0.110	2.500	0.350

Castillo, L.G., Carrillo, J.M. & Blázquez, A. (2014). Plunge pool dynamic pressures: a temporal analysis in the nappe flow case. Journal of Hydraulic Research, DOI: 10.1080/00221686.2014.968226.

Universidad Politécnica de Cartagena

ETS de Ingeniería de Caminos, Canales y Puertos y de Ingeniería de Minas

Hidr@m

Introduction | **Semi-empirical** | Experiment

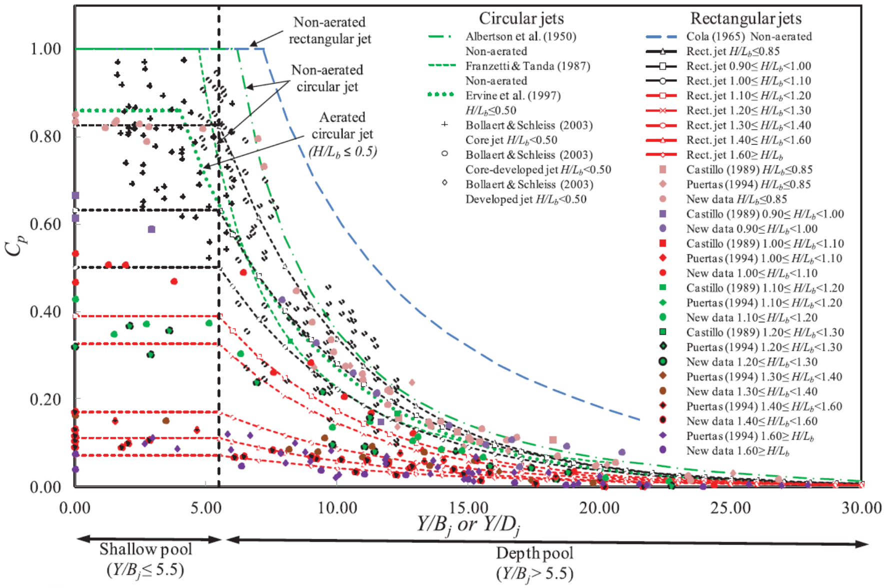

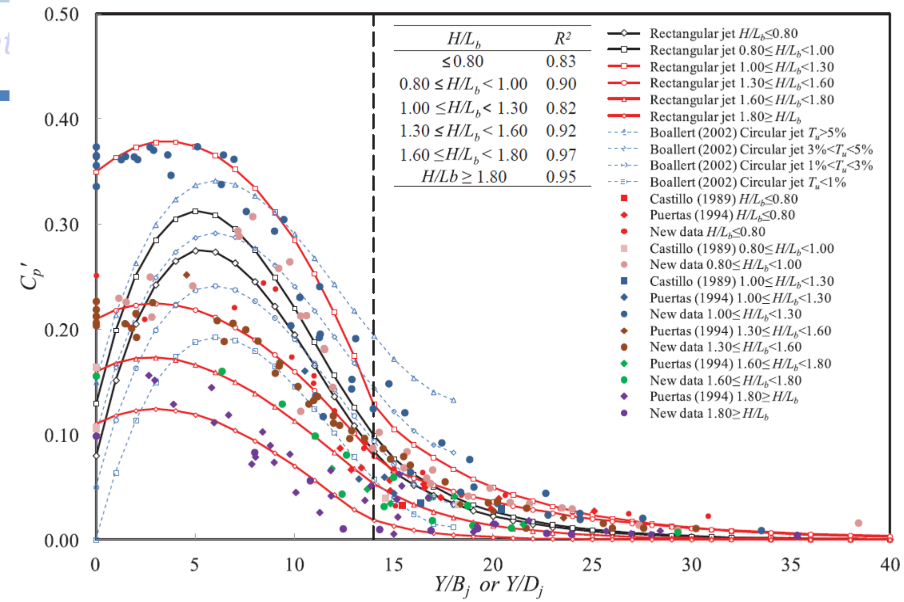

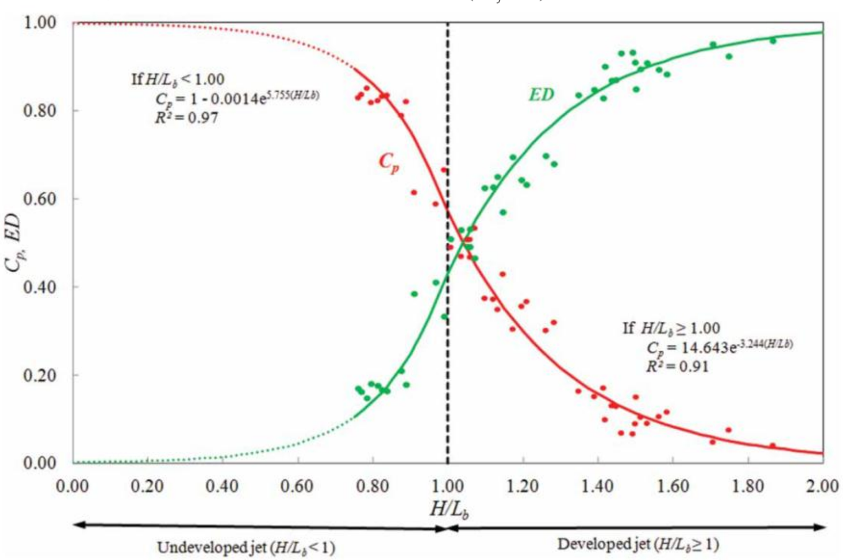

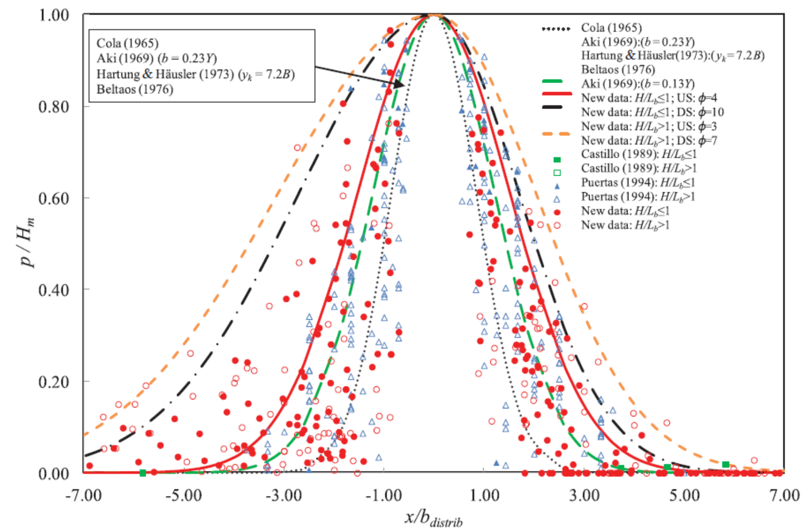

Velocity and aeration measurements
- In the plunge pool

- Within plunge pool downstream of the impingement point, the flow resembles in a submerged hydraulic jump and a wall jet.

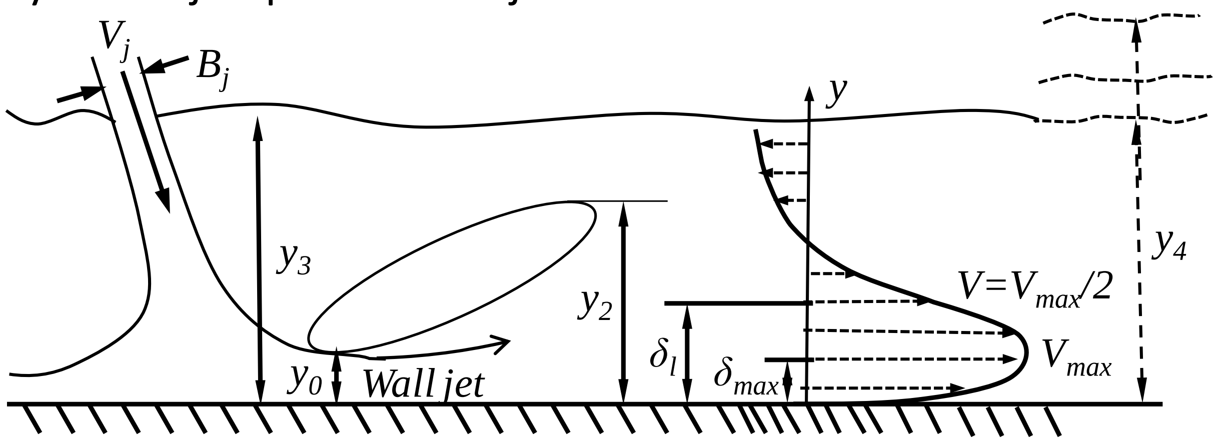

- Situation is complicated by the air entrainment. Several formulas have been put forward to obtain the horizontal velocity distribution in the vertical profile.

- Our studies shown that "homogeneous" theoretical model of ANSYS CFX is able to reproduce correctly the jet water velocity, and the averaged pressures in the plunge pool.

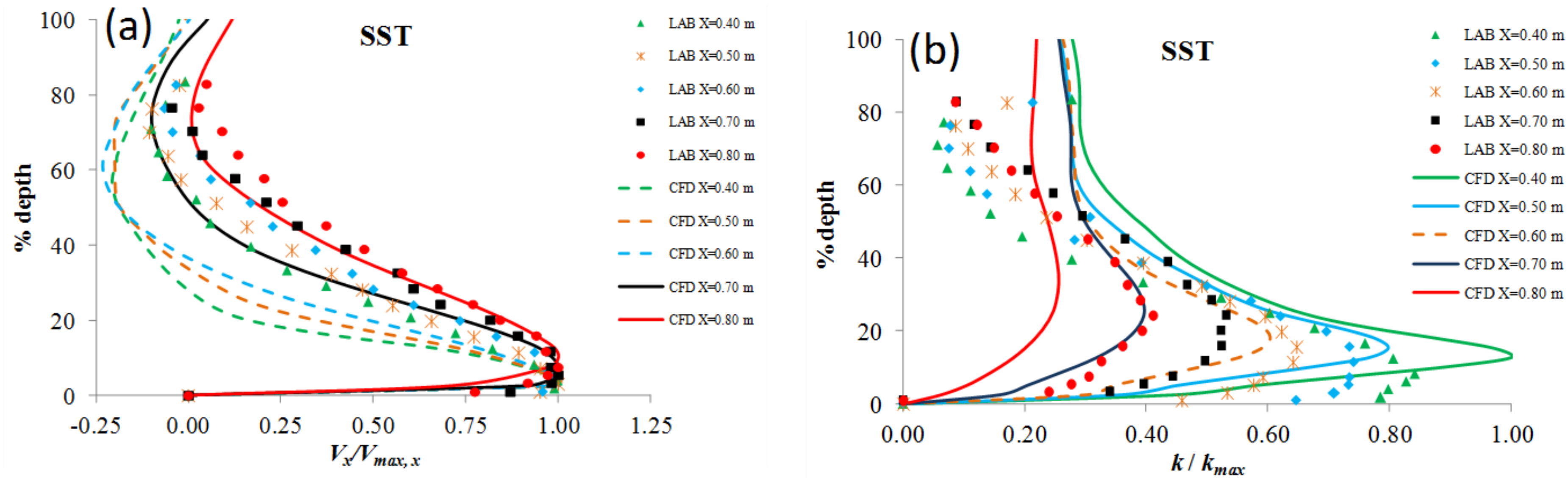

(a) Horizontal velocity profiles in plunge pool downstream of the stagnation point. (b) Turbulent kinetic energy profiles. SST model (q = 0.082 m^2/s, H = 1.993 m, Y = 0.32 m).

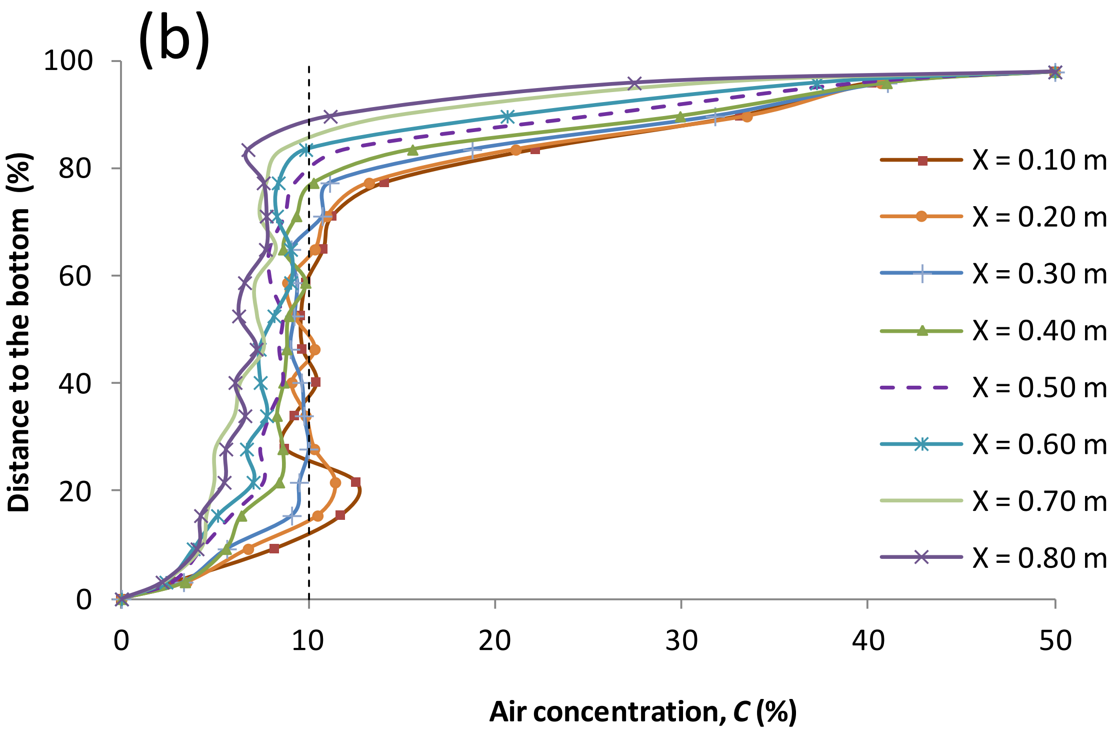

- Maximum air concentration is around 12% (distance of 21% from bottom) for the first sections. From section 0.30 m and distance from the bottom < 70%, the air concentration is <10%.

Castillo, L.G., Carrillo, J.M. & Bombardelli, F.A. (2017). Distribution of mean flow and turbulence statistics in plunge pools. Journal of Hydroinformatics, 19(2), 173-190. DOI: 10.2166/hydro.2016.044.

- **Bubble frequency and mean diameter**

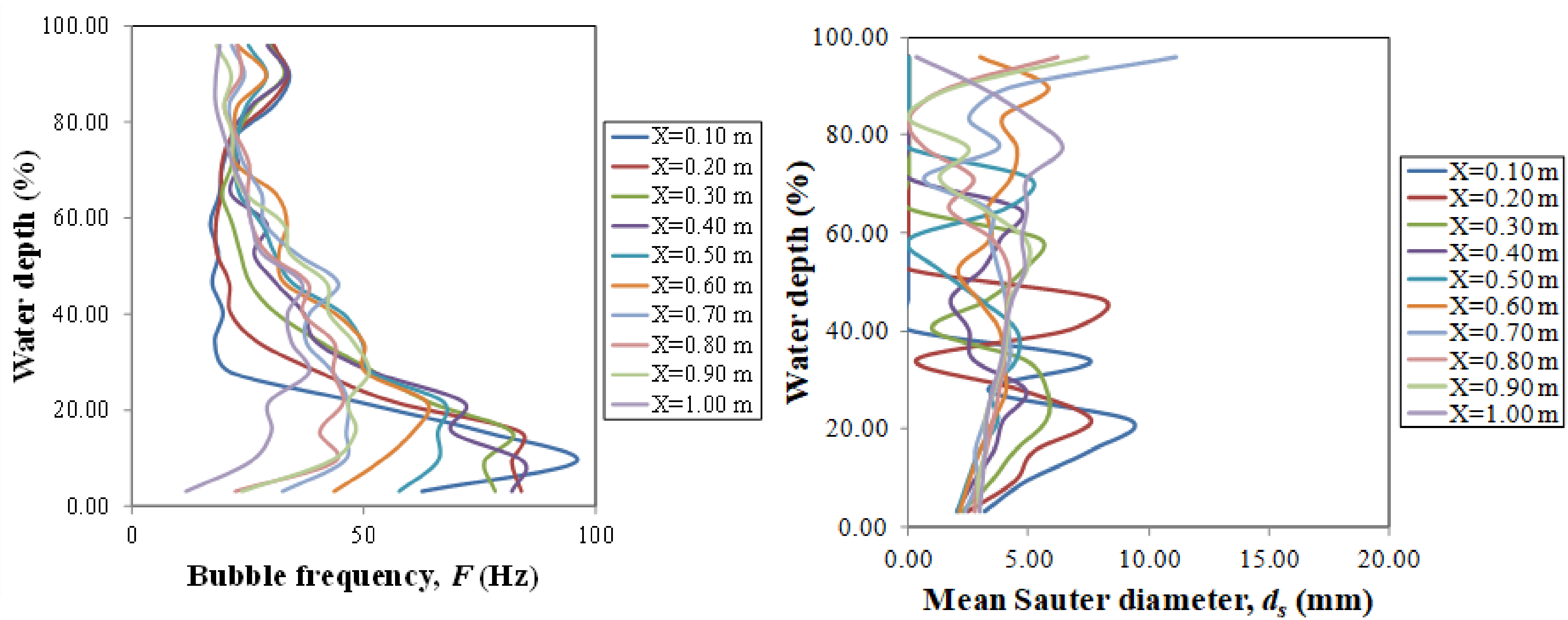

Frequency and mean diameter of bubbles detected downstream of the stagnation point (q = 0.082 m^2/s, H = 2.19, Y = 0.32 m).

Carrillo, J.M., Castillo, L.G., Marco, F. & García, J.T. (2018). 7th International Symposium on Hydraulic Structures. Aachen, Germany, 15-18 May.

- **Energy dissipation in the plunge pool**

$$\frac{H_L}{H_0} = \frac{2\left(\frac{y_3}{y_0}-\frac{y_4}{y_0}\right)+\left(1-\frac{1}{(y_4/y_0)^2}\right)F_{r0}^2}{2(y_3/y_0)+F_{r0}^2}$$

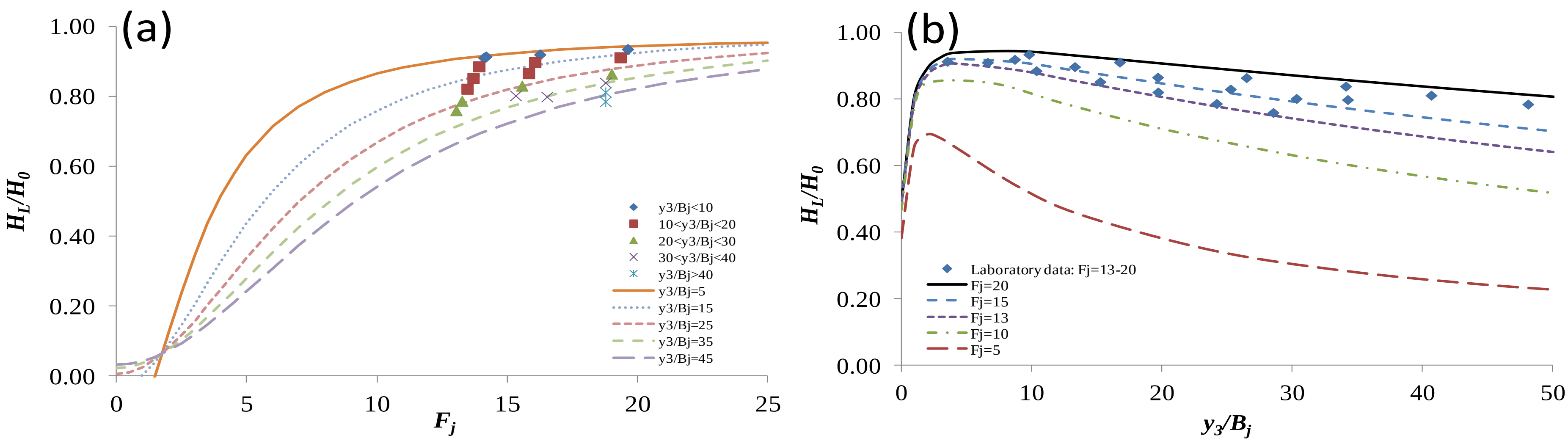

Relative energy dissipation in the plunge pool: (a) in function of the impingement. Froude number. (b) in function of the ratio y_3/B_j for the cases B_j = 0.015 m and F_j = 13-20.

Castillo, L.G., Carrillo, J.M. & Sordo-Ward, A. (2014). Simulation of overflow nappe impingement jets. Journal of Hydroinformatics, 16(4), 922-940. DOI: 10.2166/hydro.2014.109.

PAUTE CARDENILLO DAM (Ecuador)

Arch dam of 135 m height. River bed: 24 m of alluvial and 10 m of weathered rock

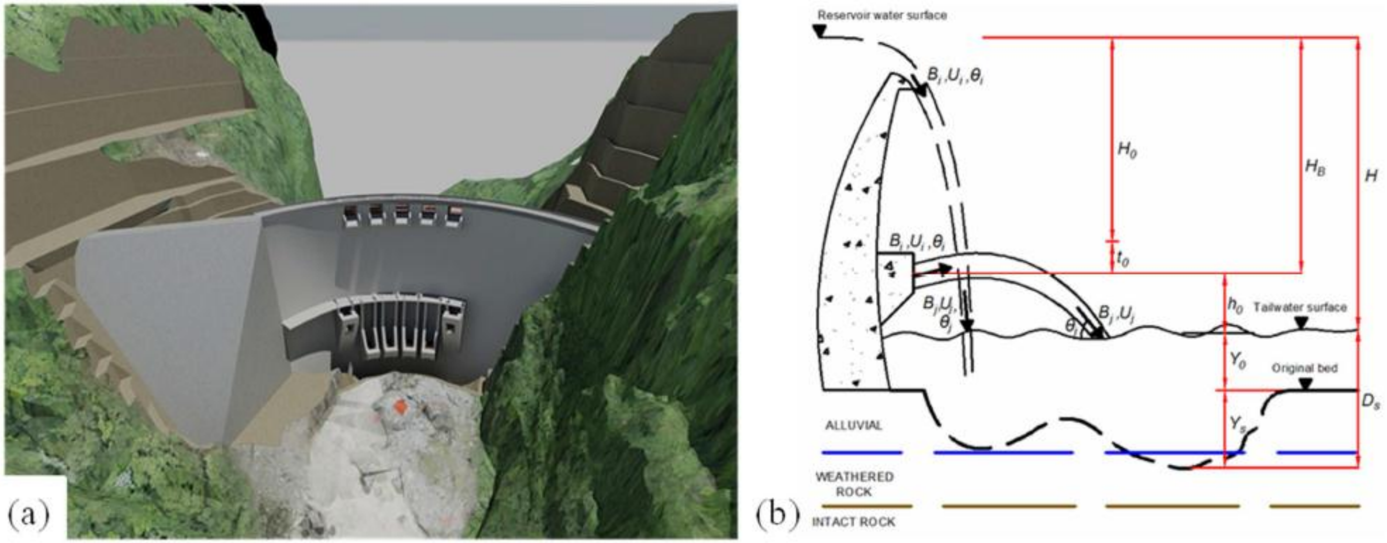

Scour due to the operation of the free surface spillway (700 m^3/s) and half-height outlets (1760 m^3/s), with complementary procedures:

- Semi-empirical methodology based on pressure fluctuations-erodibility index
- Computational fluid dynamics simulations (CFD)

Bed Material	D_{16} (m)	D_{50} (m)	D_{84} (m)	D_{90} (m)	D_m (m)
Alluvial (820 MASL to 796 MASL)	0.006	0.150	0.225	0.240	0.124
Weathered rock (796 MASL to 786 MASL)	0.045	0.160	0.500	0.550	0.235

Castillo, L.G. & Carrillo (2016). Scour, Velocities and Pressures Produced by Spillway and Outlets of Dam. Water, 8, 68; doi:10.3390/w8030068.

Semi – Empirical Methodology

Erodibility index is based on an erosive threshold that relates the magnitude of relative erosion capacity of water and the relative capacity of a material to resist scour.

Annandale (1995, 2006) summarized and established a relationship between the stream power and the erodibility index for a wide variety of materials and flow conditions. Stream power per unit of area available of an impingement jet is:

$$P_{jet} = \frac{\gamma QH}{A}$$

γ: specific weight of water
Q: flow discharge
H: fall height or the upstream energy head
A: jet area on the impact surface.

The erodibility index is defined as:

$$K = M_s K_b K_d J_s$$

M_s: number of resistance of the mass; K_b: number of the block size
K_d: number of resistance to shear strength on the discontinuity contour
J_s: number of structure relative of the grain.

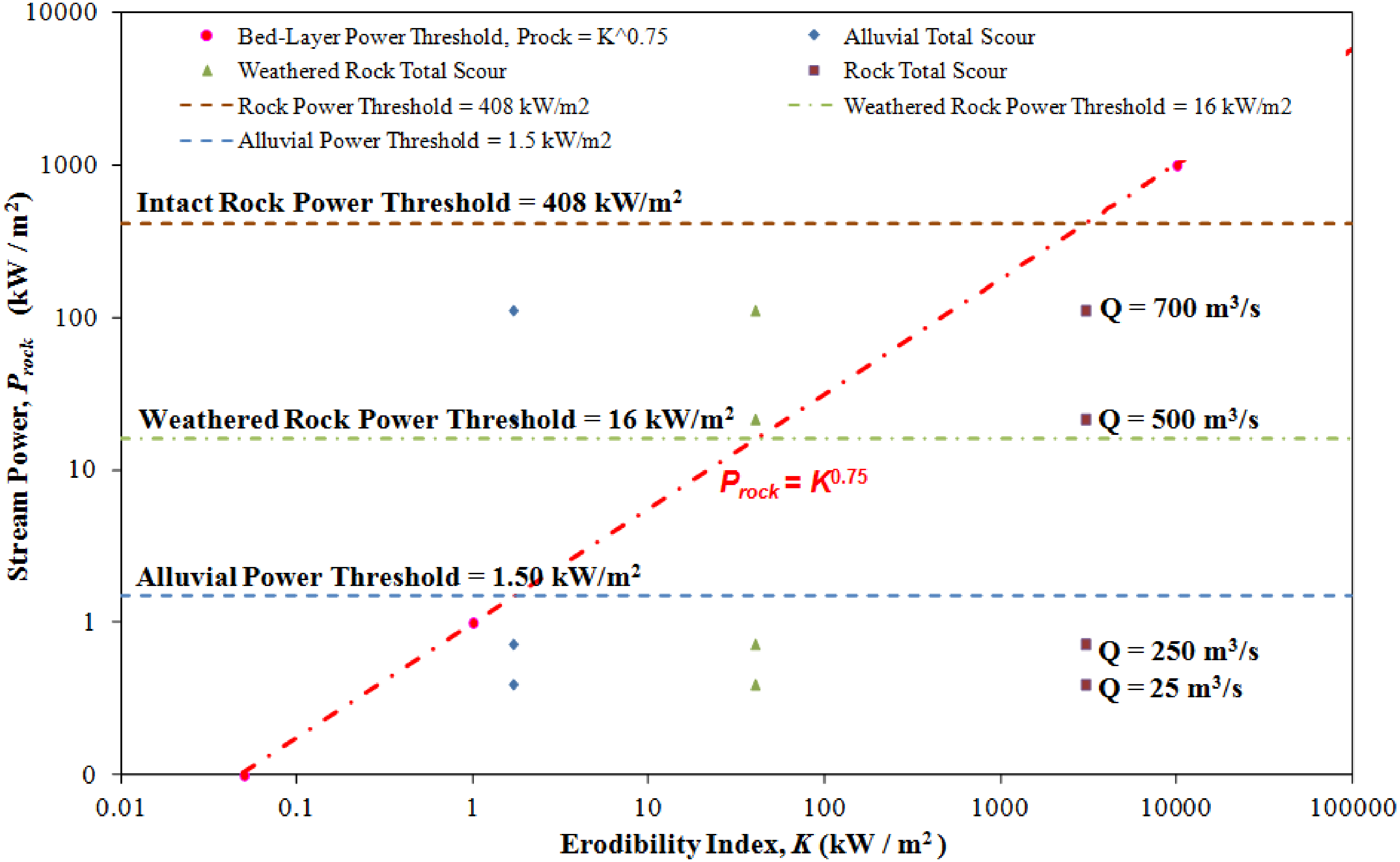

Stream power of the jet for different flows as a function of the erodibility.
Alluvial, weathered rock and intact rock indexes (Ys = 18 m, Y0 = 6 m) for the free surface weir.

Simulation with FLOW-3D

Table 8. Principal relations to calculate the sediment scour model in FLOW-3D.

Relation	Formulae
Drag function	$K_i = \frac{3}{4}\frac{f_{s,i}}{d_{s,i}}\left(\rho_f C_{D,i}\|\mathbf{u}_{r,i}\| + 24\frac{\mu_f}{d_{s,i}}\right)$
Drift velocity correction	$\mathbf{u}_{r,i}^{eff} = \mathbf{u}_{r,i}(1-f_s)^{\zeta}$
Richardson-Zaky coefficient	$\zeta_0 = 4.35$ for $R_e < 0.2$ $\zeta_0 = 4.35/R_e^{0.03}$ for $0.2 < R_e < 1.0$ $\zeta_0 = 4.45/R_e^{0.1}$ for $1.0 < R_e < 500$ $\zeta_0 = 2.39$ for $R_e > 500$
Critical Shields parameter (S-W) *	$\theta_{cr,i} = \frac{0.3}{1+1.2R_i^*} + 0.055\left[1-\exp(-0.02R_i^*)\right]$
Critical Shields parameter modified for sloping surface	$\theta'_{cr,i} = \theta_{cr,i}\frac{\cos\Psi\sin\beta + \sqrt{\cos^2\beta\tan^2\phi_i - sen^2\Psi sen^2\beta}}{\tan\phi_i}$
Local Shields number	$\theta_i = \frac{\tau}{\|g\| d_{s,i}(\rho_{s,i}-\rho_f)}$
Sediment entrainment lift velocity	$\mathbf{u}_{lift,i} = \alpha_i \mathbf{n}_s d_*^{0.3}\left(\theta_i - \theta'_{cr,i}\right)^{1.5}\sqrt{\frac{\|g\| d_{s,i}(\rho_{s,i}-\rho_f)}{\|g\| d\rho_f}}$
Dimensionless particle diameter	$d_* = d_{s,i}\left[\frac{\rho_f(\rho_{s,i}-\rho_f)\|g\|}{\mu_f^2}\right]^{\frac{1}{3}}$
Volumetric bed-load transport rate per unit width	$q_{b,i} = f_{b,i}\Phi_i\left[\|g\|\left(\frac{(\rho_{s,i}-\rho_f)}{\rho_f}\right)d_{s,i}^3\right]^{\frac{1}{2}}$
Bed-load thickness	$\frac{\delta_i}{d_{s,i}} = 0.3d_*^{0.7}\left(\frac{\theta_i}{\theta'_{cr,i}} - 1\right)^{0.5}$

Parameters

$d_{s,i}$ and $C_{D,i}$ = diameter and drag coefficient for sediment species i
μ_f = fluid dynamic viscosity
$\mathbf{u}_{r,j}$ = drift velocity
f_s = sediment total volume fraction
$\zeta = \zeta_{user}\zeta_0$; $\zeta_{user} = 1$
$R_e = \rho_f d_i \|\mathbf{u}_{r,i}\|/\mu_f$ = Reynolds number on the particle d_i
ρ_f = fluid density
$R_i^* = d_{s,i}\frac{\sqrt{0.1(\rho_{s,i}-\rho_f)\rho_f\|g\| d_{s,i}}}{\mu_f}$
$\rho_{s,i}$ = density of sediment species i
β = slope bed angle
ϕ_i = repose angle for sediment species i (default is 32°)
Ψ = angle between the flow and the upslope direction (flow directly up a slope $\Psi = 0°$)
τ = local shear stress
$\|g\|$ = gravitational vector
α_i = entrainment parameter (~0.018)
$\mathbf{n}_s$ = outward pointing normal to the packed bed interface
$f_{b,i}$ = volume fraction of sediment i in the bed-load layer
Φ_i = dimensionless bed-load transport (MPM) **
d_* = dimensionless particle diameter
θ_i = local Shields number

* Soulsby and Whitehouse equation; ** Meyer-Peter and Müller equation.

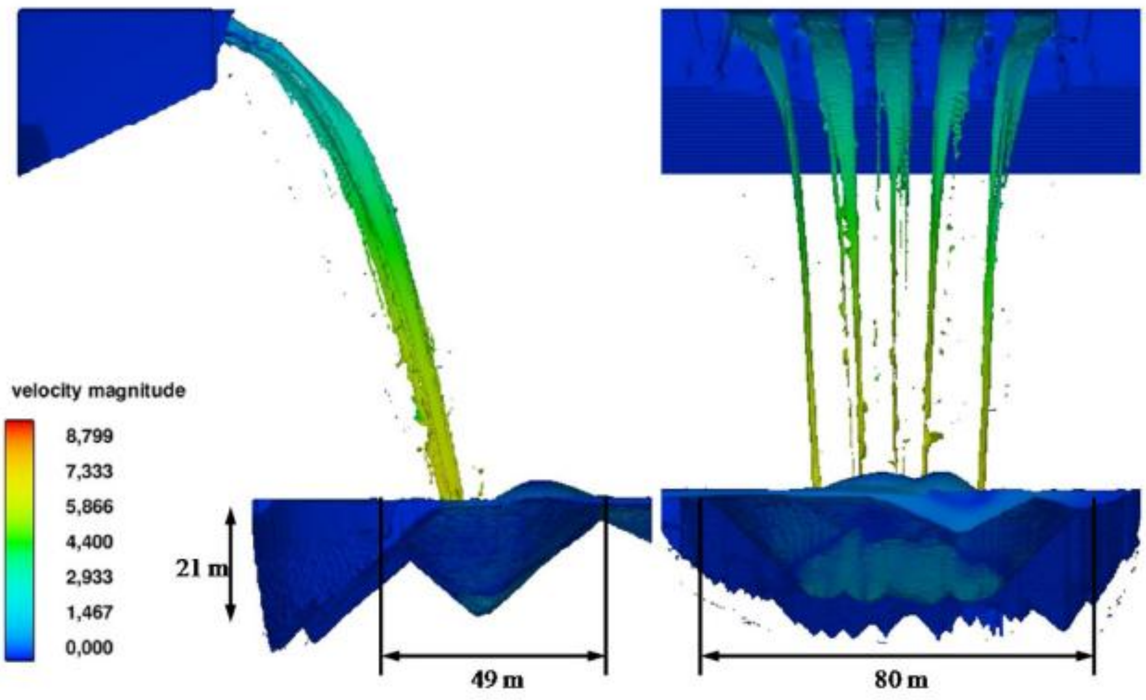

Figure 11. Scour bowl due to the free surface weir jet. Bilayer simulation: alluvial 24 m and weathered rock 10 m (Units in m/s. Froude scale 1:50. Prototype impingement velocity = $6.1 \times 50^{1/2} = 43.13$ m/s).

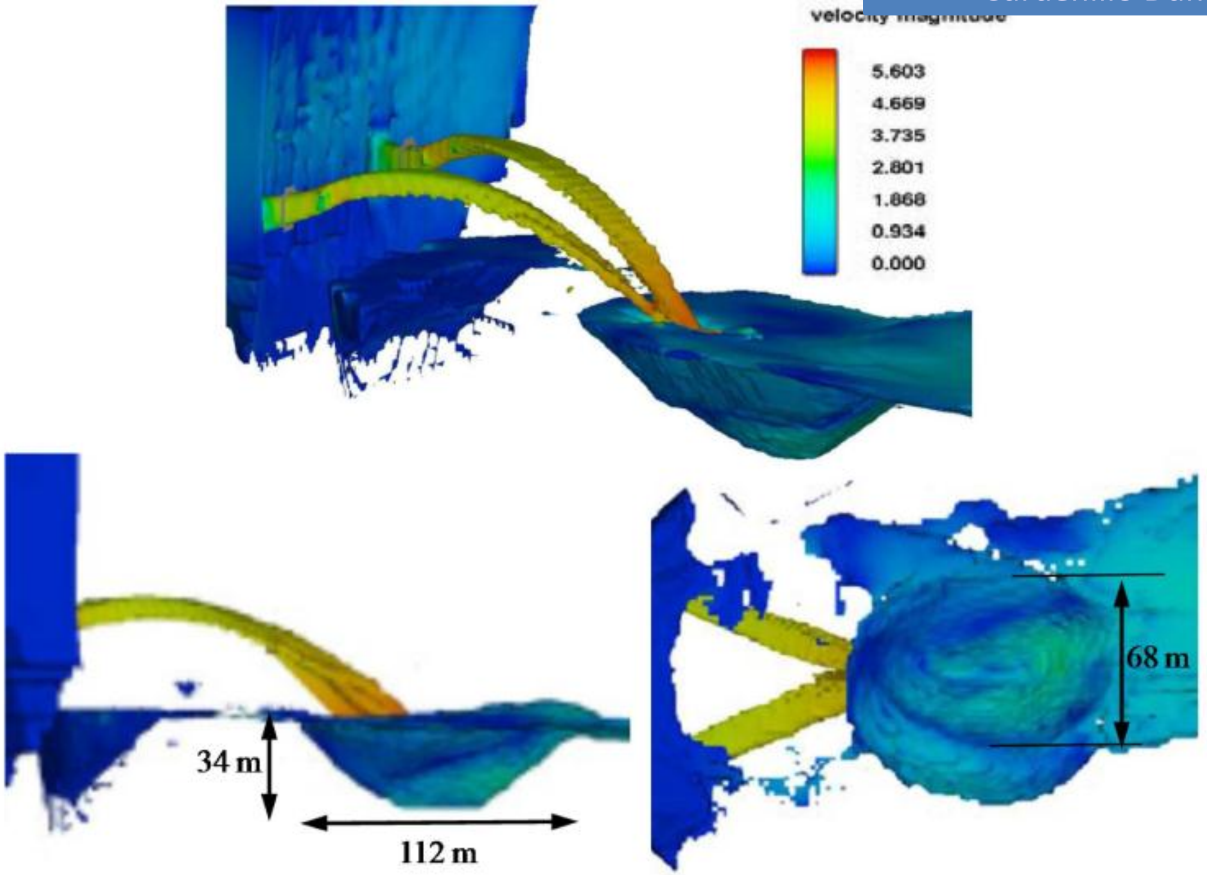

Figure 12. Scour bowl due to the half-height outlet. Bilayer simulation: alluvial 24 m and weathered rock 10 m. (Units in m/s. Froude scale 1:50. Prototype impingement velocity = $5.4 \times 50^{1/2} = 38.18$ m/s).

Table 9. Comparison of scour obtained by different methods for free surface weir and half-height outlet.

Method	Free Surface Weir Q_4 = 700 m^3/s			Half-Height Outlet Q_{40} = 1760 m^3/s		
	Y_s (m)	Y_s + 0.50SD (m)	Y_s + SD (m)	Y_s (m)	Y_s + 0.50SD (m)	Y_s + SD (m)
Empirical formulations	17	24	34	32	>34	>34
Erodibility Index Pressure fluctuations	20	-	-	>34	-	-
FLOW-3D v11	21	-	-	>34	-	-

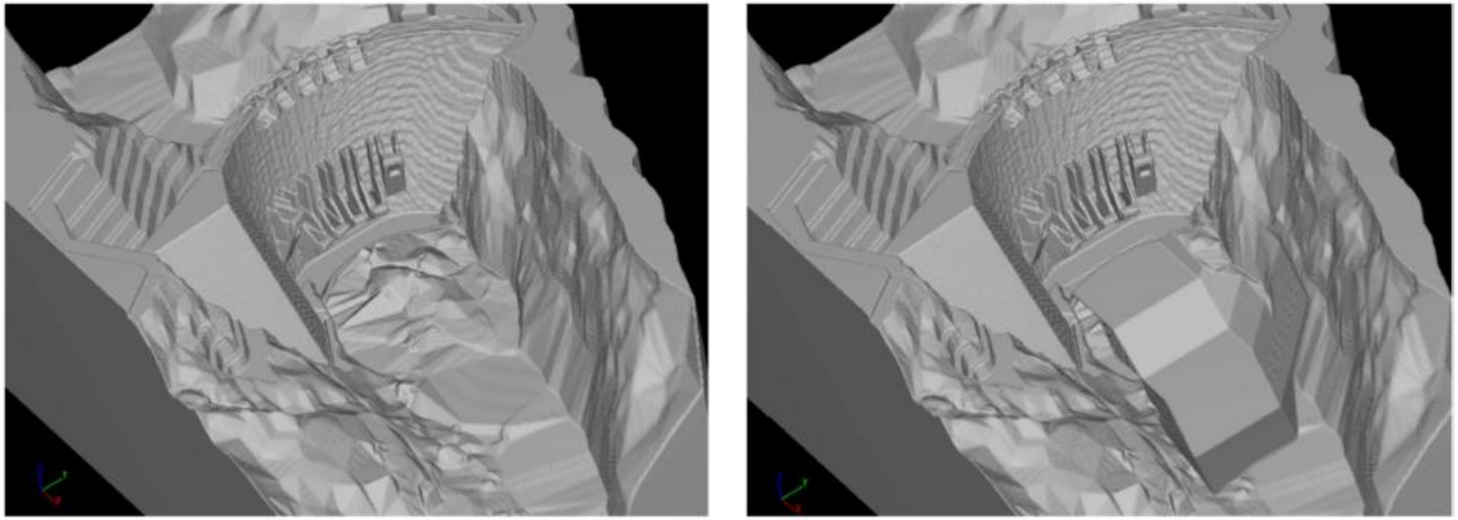

(a) (b)

Figure 13. Pre-excavated basin. (**a**) Initial condition; (**b**) geometry proposed.

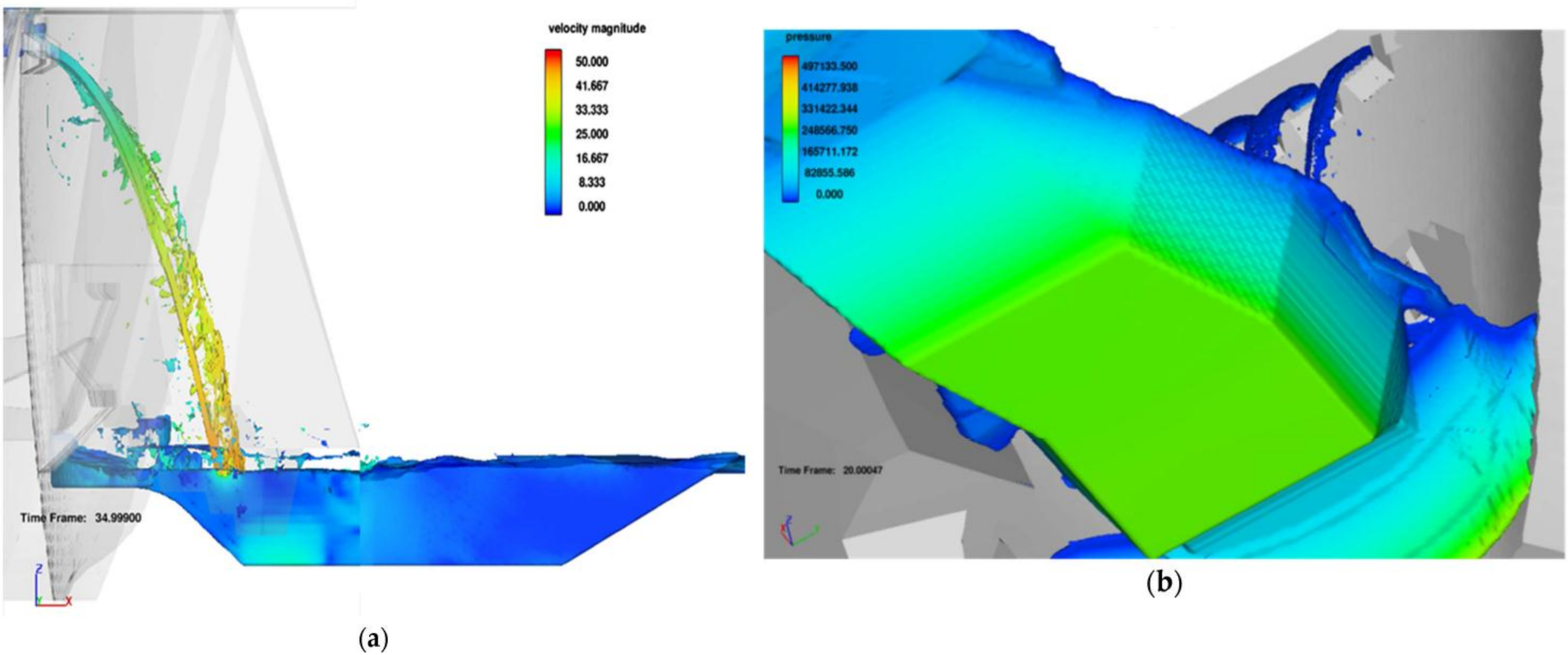

Figure 14. Lateral and spatial views of the free surface weir jets in the air and in the pre-excavated stilling basin (Prototype scale. Units in m/s and in Pascal): (a) Velocities; (b) Pressures (Q = 700 m^3/s).

TOACHI DAM (Ecuador)

Concrete dam of 59 m height and 0.3/1.0 and 0.7/1.0 (horizontal/vertical).

- Spillways end in a ski jump and they have two baffles to divide the flow
- Q_{1000} =1213 m^3/s (Hidrotoapi, 2010)

Three-dimensional view and 1:50 scale physical model (EPN, 2013).

Castillo, L.G., Castro, M., Carrillo, J.M., Hermosa, D., Hidalgo, X., & Ortega, P. (2016). Experimental and numerical study of scour downstream Toachi Dam. Sustainable Hydraulics in the Era of Global Change - Proceedings of the 4th European Congress of the International Association of Hydroenvironment Engineering and Research, 519-526.

- River bed was modeled considering a uniform crushed gravel size whose mean value was 0.020 m in the scale model (1.00 m in the prototype).

- The mobile bed was 2.10 m long and 1.36 m wide in the model. Erodible layer = 0.40 m.

- The scour downstream of the dam was analyzed by using different flows. Flow simulation time = 90 min.

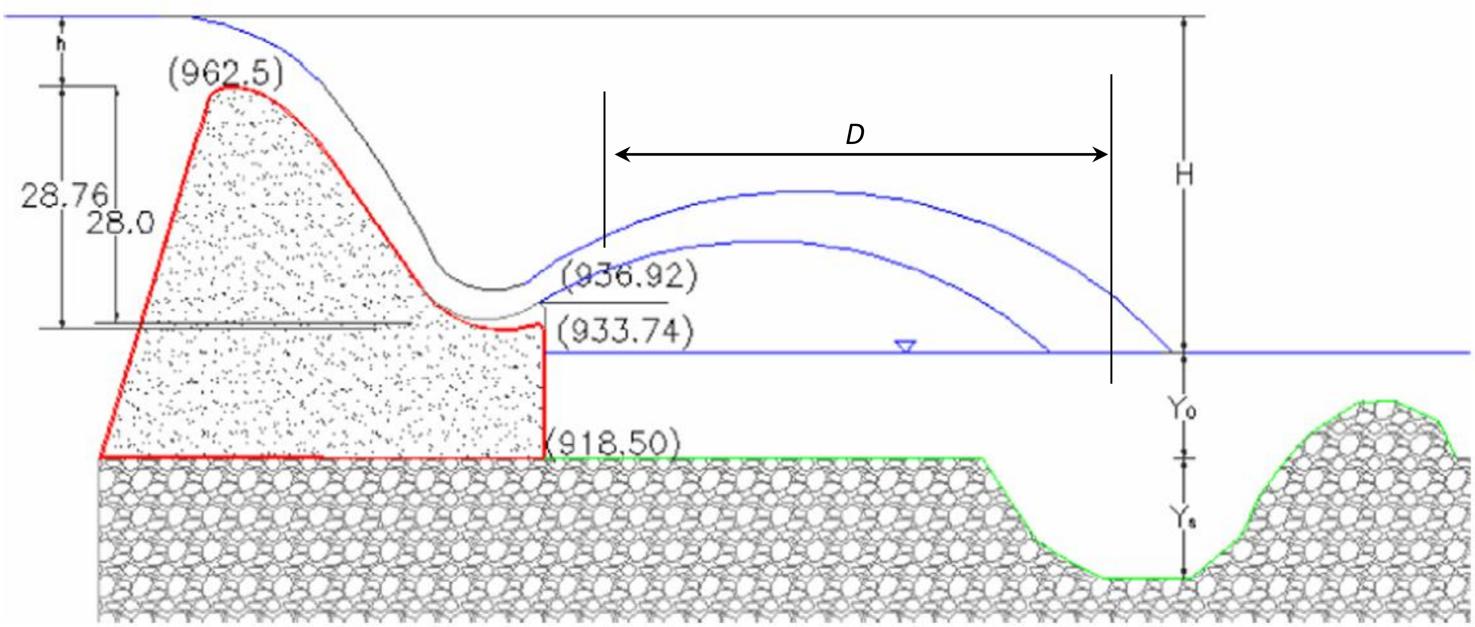

Parameters of the threshold of rock strength.

d_{50}	d_{84}	θ	M_s	K_b	K_d	J_s	K	P_{rock}
(m)	(m)	(°)	(-)	(-)	(-)	(-)	(-)	(kW/m^2)
1.02	1.2	36	0.41	1061.21	0.73	1.00	316.12	74.97

Impingement stream power (P_{jet}) and reduced stream power by diffusion in the water cushion [P_{jet} (Y/B_j)].

Q	Y_s	Y_0	Y_0+Y_s	P_{jet}	P_{jet} (Y/B_j)
(m^3/s)	(m)	(m)	(m)	(kW/m^2)	(kW/m^2)
264	6.57	5.47	12.05	76.94	3.72
500	8.05	7.75	15.80	94.26	19.79
711	7.05	8.68	15.70	101.59	43.6
999	7.15	12.25	19.40	113.02	71.5
1213	6.65	12.00	18.65	108.31	64.59

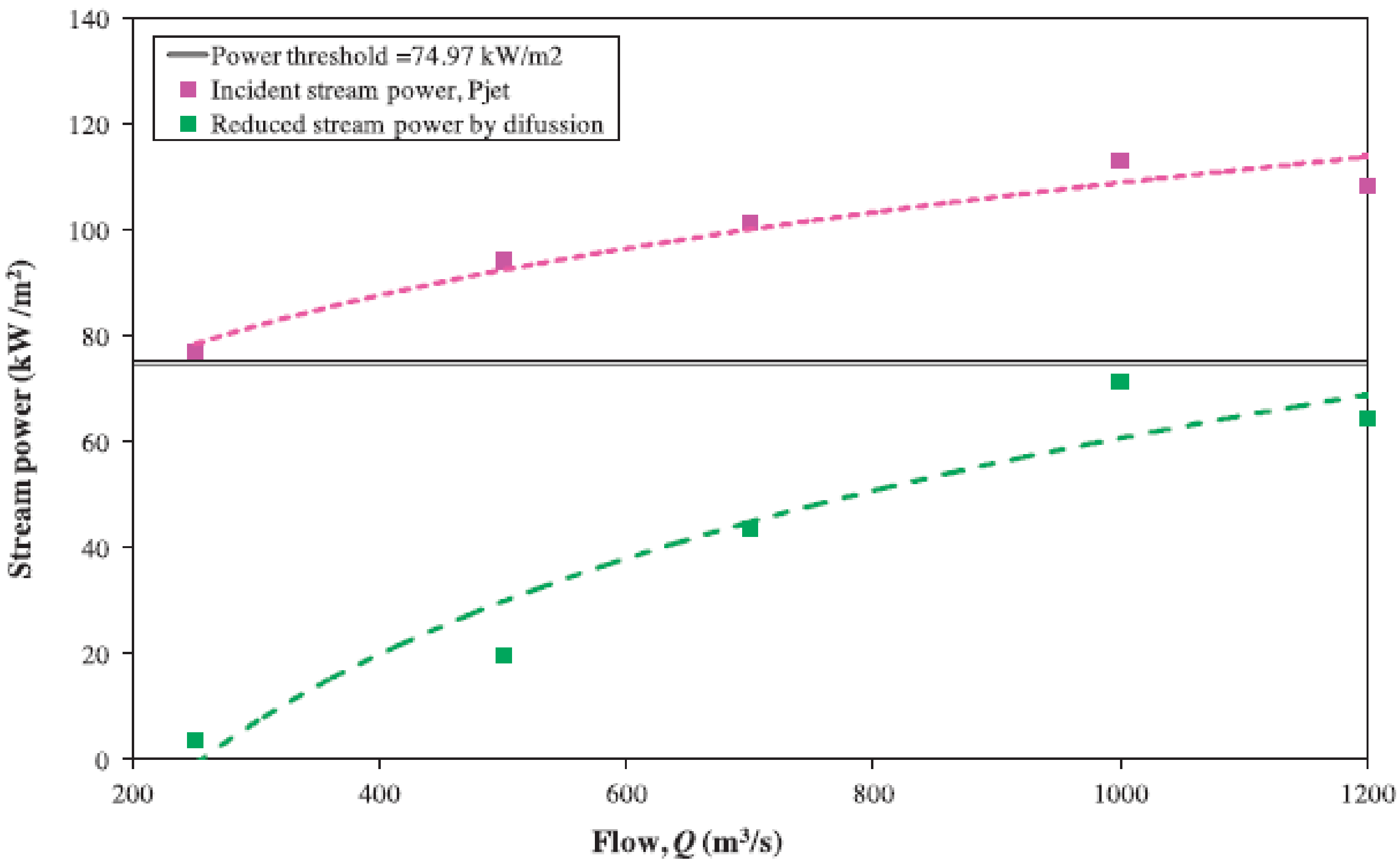

Fig. 9. Incident stream power P_{jet} and reduced stream power by diffusion $P_{jet}\ (Y/B_j)$ of the jet.

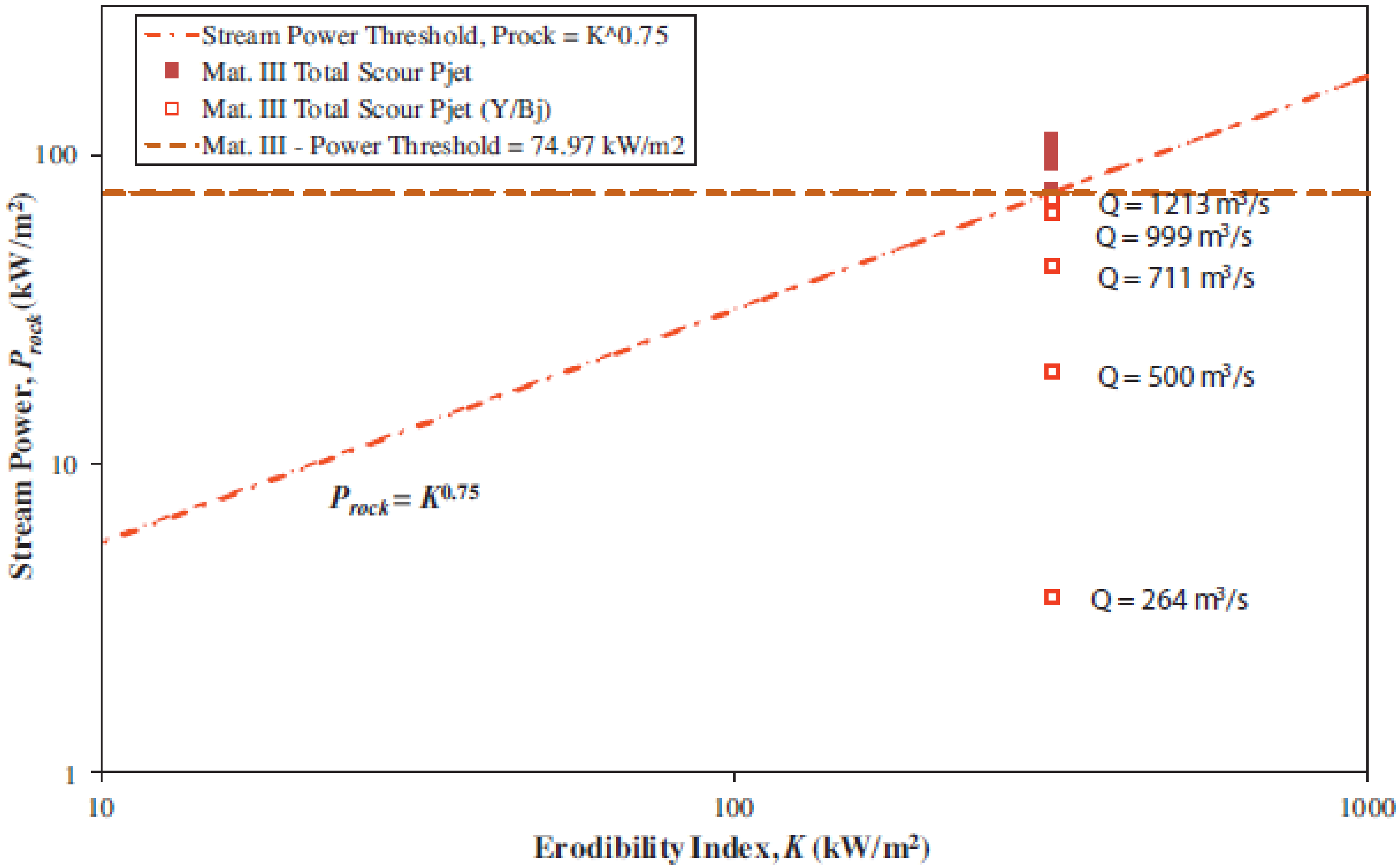

Fig. 10. Stream power of the jet for different flows as a function of the erodibility.

Simulation with FLOW-3D

Dimensionless bed-load transport (MPM):

$$\Phi_i = \beta_i(\theta_i - \theta'_{cr,i})^{1.5}$$

$\beta_i = 8$
(5 and 13 for low and high sediment transport)

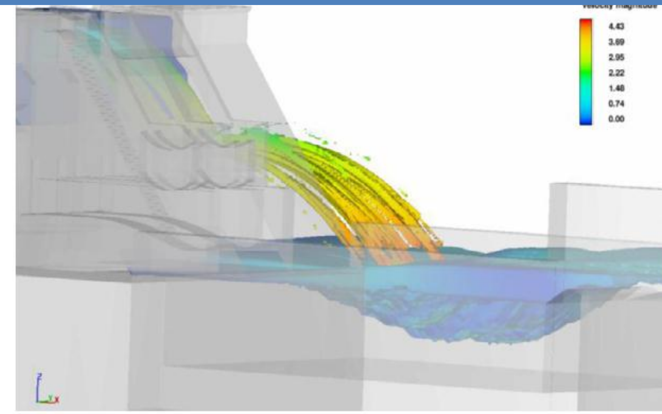

Fig. 11. Velocities magnitude of the flow and scour downstream of the Toachi Dam for the design flow (Q = 1213 m³/s).

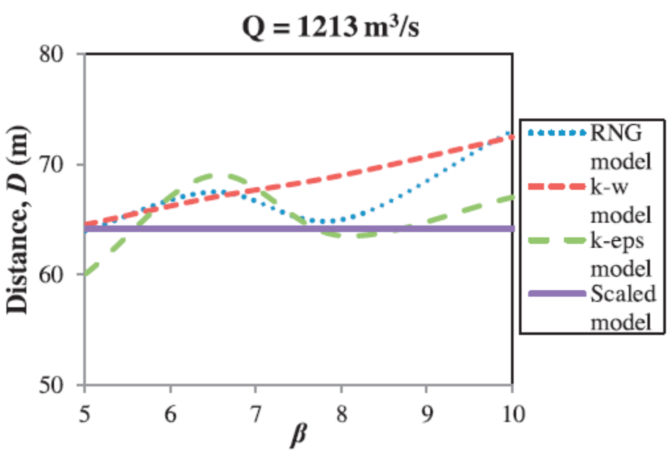

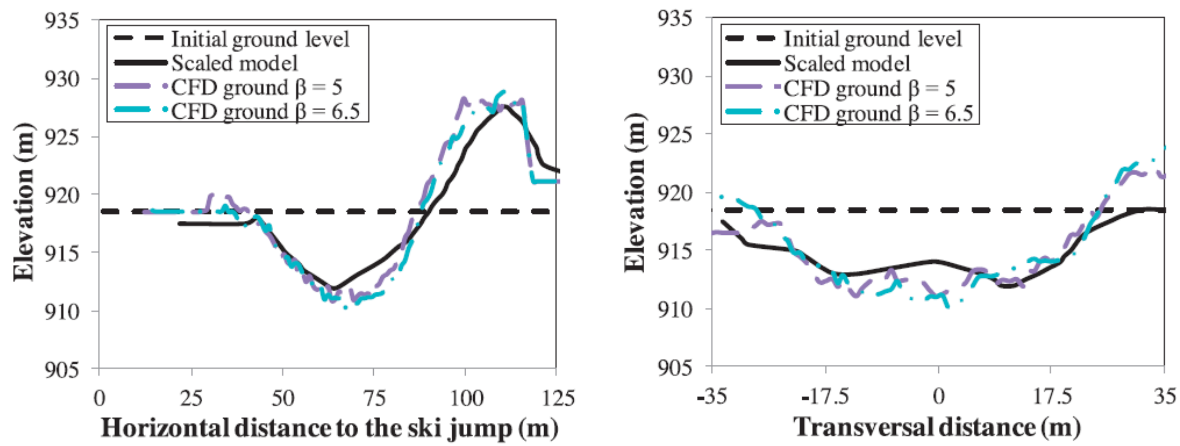

Fig. 14. Longitudinal and transversal scour shape measured and simulated.

Castillo, L.G., & Carrillo, J.M. (2017). Comparison of methods to estimate the scour downstream of a ski jump. International Journal of Multiphase Flow, 92, 171-180. DOI: 10.1016/j.ijmultiphaseflow.2017.03.006.

CONCLUSIONS

- Observing and predicting two-phase flows in hydraulic structures is very complicated due to the rather non-dilute nature of the flow. Under these conditions, both experiments and simulations cannot be expected to lead to clean comparisons.

- In general, the CFD simulations of air-water flows provide results fairly close to the values measured in the laboratory, in spite of having used simple two-phase flow models. However, in the highly aerated regions rather strong differences appear.

- In the scour downstream of a dam, it is required to compare and contrast the results obtained with several procedures. Once calibrated, CFD simulations allow to obtain a better knowledge of the process.

FUTURE DEVELOPMENTS

- Obtain dynamic pressures coefficients to $H/L_b < 0.50$. By means of pumping system and rectangular nozzle (velocities over 20 m/s).

- Measurements in prototype.